

# Structural Basis of Substrate Specificity and Regiochemistry in the MycF/TyIF Family of Sugar O-Methyltransferases.

Steffen M. Bernard,<sup>†,‡</sup> David L. Akey,<sup>‡</sup> Ashootosh Tripathi,<sup>‡</sup> Sung Ryeol Park,<sup>‡</sup> Jamie R. Konwerski,<sup>‡</sup> Yojiro Anzai,<sup>§</sup> Shengying Li,<sup>‡</sup> Fumio Kato,<sup>§</sup> David H. Sherman,<sup>‡,||</sup> and Janet L. Smith<sup>\*,‡,⊥</sup>

<sup>†</sup>Chemical Biology Doctoral Program, University of Michigan, Ann Arbor, Michigan 48109, United States

<sup>‡</sup>Life Sciences Institute, University of Michigan, Ann Arbor, Michigan 48109, United States

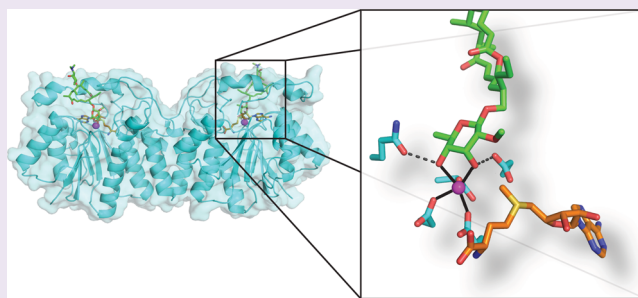
<sup>§</sup>Faculty of Pharmaceutical Sciences, Toho University, 2-2-1 Miyama, Funabashi, Chiba 274-8510, Japan

<sup>||</sup>Departments of Medicinal Chemistry, Chemistry, and Microbiology & Immunology, University of Michigan, Ann Arbor, Michigan 48109, United States

<sup>⊥</sup>Department of Biological Chemistry, University of Michigan, Ann Arbor, Michigan 48109, United States

## Supporting Information

**ABSTRACT:** Sugar moieties in natural products are frequently modified by O-methylation. In the biosynthesis of the macrolide antibiotic mycinamicin, methylation of a 6'-deoxyallose substituent occurs in a stepwise manner first at the 2'- and then the 3'-hydroxyl groups to produce the mycinose moiety in the final product. The timing and placement of the O-methylations impact final stage C-H functionalization reactions mediated by the P450 monooxygenase MycG. The structural basis of pathway ordering and substrate specificity is unknown. A series of crystal structures of MycF, the 3'-O-methyltransferase, including the free enzyme and complexes with S-adenosyl homocysteine (SAH), substrate, product, and unnatural substrates, show that SAM binding induces substantial ordering that creates the binding site for the natural substrate, and a bound metal ion positions the substrate for catalysis. A single amino acid substitution relaxed the 2'-methoxy specificity but retained regiospecificity. The engineered variant produced a new mycinamicin analog, demonstrating the utility of structural information to facilitate bioengineering approaches for the chemoenzymatic synthesis of complex small molecules containing modified sugars. Using the MycF substrate complex and the modeled substrate complex of a 4'-specific homologue, active site residues were identified that correlate with the 3' or 4' specificity of MycF family members and define the protein and substrate features that direct the regiochemistry of methyltransfer. This classification scheme will be useful in the annotation of new secondary metabolite pathways that utilize this family of enzymes.



Natural products are a valuable source of pharmacologically active compounds.<sup>1</sup> The large number of stereocenters and complex architecture make many natural products challenging targets for chemical synthesis. Chemoenzymatic and bioengineering methods to generate new secondary metabolites are becoming more versatile and have shown promise for expanding chemical diversity.<sup>2-4</sup> While conceptually straightforward, effective use of these emerging biosynthetic approaches relies on knowledge of the substrate specificity and reaction mechanism for each enzyme. Catalysts for methylation at defined positions on specific sugar residues are likely to be useful chemoenzymatic tools as they are commonly incorporated into macrolide natural products.<sup>5</sup> Modifications, including O-, N-, and C-methylations; acetylation; oxidation; and epimerization, result in a diverse array of sugars not observed in primary metabolism.<sup>6</sup> Modifications alter the ability of macrolide natural products to interact with targets and impact their solubility and membrane permeability.

Some natural product sugar O-methyltransferases can function *in vitro* on non-natural substrates,<sup>7</sup> and aided by high-resolution structures of substrate complexes, we anticipate the ability to more accurately assess the flexibility and specificity of this important group of enzymes.

Sugars are incorporated into natural products as nucleotide mono- or diphosphate conjugates derived from glucose or fructose, most commonly as thymidine diphosphate (TDP) activated forms.<sup>6</sup> TDP-sugars are frequently modified through epimerization, dehydration, reduction, amination, or methylation and subsequently transferred to natural product scaffolds by glycosyltransferases.<sup>8</sup> Once incorporated, additional modifications including O- and N-methylation or acetylation are common. Enzymes that catalyze TDP-sugar modification, many

Received: November 27, 2013

Accepted: February 18, 2015

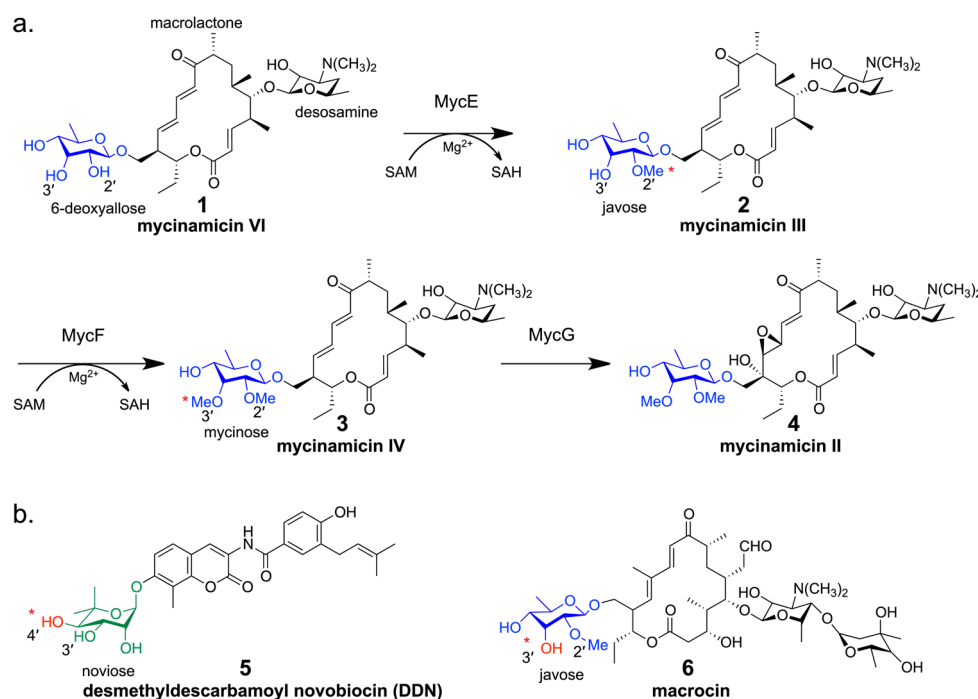


**Figure 1.** Sugar methylation in natural product biosynthesis. (a) Ordered sugar *O*-methylation in the mycinamicin pathway. MycE catalyzes the 2'-*O*-methylation of the 6'-deoxyallose of mycinamicin VI 1 to generate the javose of mycinamicin III 2. MycF catalyzes the 3'-*O*-methylation of javose to form the mycinose of mycinamicin IV 3. The P450 monooxygenase, MycG, catalyzes hydroxylation and epoxide ring formation to produce the final product mycinamicin II 4. (b) Substrates for the 4'-*O*-methyltransferase NovP, desmethyldescarbamoyl novobiocin 5, and the 3'-*O*-methyltransferase TylF, macrocin 6. Modified sugars are highlighted in blue or green, and sites of methylation are denoted with red asterisks.

of which have been structurally and functionally characterized,<sup>5,9</sup> may be particularly valuable in pathway engineering as they use the common TDP nucleotide to select substrates. In contrast, sugar modifying enzymes that act after glycosyl transfer may interact with functional groups specific to their substrates. Moreover, the utility of downstream sugar methyltransferases in design or engineering of new metabolic pathways is unknown, as structural or functional information on their interaction their substrates is limited.

Mycinamicins are produced by *Micromonospora griseorubida* and are a clinically promising group of macrolide antibiotics because they exhibit greater activity against antibiotic-resistant bacterial strains than do clinically used antibiotics.<sup>10,11</sup> The mycinamicin 16-membered macrolactone core has two *O*-linked modified sugars. The mycinose sugar is derived from 6'-deoxyallose. Following transfer to the macrolide core, the sugar is modified sequentially by two magnesium- and *S*-adenosylmethionine (SAM)-dependent methyltransferases. MycE methylates the 2'-hydroxyl of 6'-deoxyallose to form javose and MycF methylates javose at the 3' position to generate the mycinose sugar (Figure 1).<sup>12</sup> MycE and MycF catalyze essentially the same reaction but are highly selective for their respective substrates. Specifically, MycE catalyzes methyltransfer to the 2' sugar hydroxyl group, while MycF transfers a methyl to the 3' hydroxyl of a sugar that already bears a 2' methoxy group. The distantly related MycE and MycF belong to different branches of the class-I methyltransferase family. Each has dozens of homologues in annotated bacterial secondary metabolite pathways that catalyze sugar methylation in macrolide, anthracycline, and aminocoumarin antibiotics as well as glycopeptidolipids.<sup>13–19</sup> We previously reported crystal structures of MycE in binary and ternary complexes with a cosubstrate and substrate.<sup>20</sup> All characterized MycF subfamily

members methylate at the 3' or 4' hydroxyl positions.<sup>21,22</sup> Within this subfamily, the substrate- and metal-free structure of NovP<sup>23</sup> and the kinetic mechanism of the homologue TylF<sup>24,25</sup> have been reported; however the structural basis of substrate specificity and regioselectivity is unknown.<sup>20,23</sup> Recent structures of natural product sugar methyltransferases, including TcaB9,<sup>26</sup> RebM,<sup>27</sup> CalS11,<sup>28</sup> MycE,<sup>20</sup> and the MycF homologue NovP,<sup>23</sup> reveal a diverse array of scaffolds, as might be expected, given their highly divergent sequences. They share the Rossmann-like fold common to class-I methyltransferases but differ in the elaborations that form oligomer interfaces and confer substrate specificity.<sup>5</sup> Notably, few of these structures include relevant substrates. Here, we report a series of nine crystal structures with corresponding biochemical analysis that provide insights into substrate specificity, pathway ordering, and mechanism of MycF that is critical for construction of the fully elaborated macrolide antibiotic mycinamicin II 4.<sup>29,30</sup> Furthermore, we demonstrate the utility of a structure-guided protein engineering approach to generate a new macrolide antibiotic, 3'-methoxy-mycinamicin VI 7.

## RESULTS AND DISCUSSION

In order to understand MycF substrate specificity, we determined crystal structures (Table 1) for nine different states of the protein, including the free enzyme, a binary complex with *S*-adenosylhomocysteine (SAH), and four ternary complexes with SAH and the substrate (mycinamicin III, 2), the product (mycinamicin IV, 3), an earlier pathway intermediate (mycinamicin VI; natural MycE substrate, 1), a non-natural substrate from the related tylosin pathway (macrocin, 6), and three complexes of a MycF variant. Crystals of wild type MycF diffracted with streaky patterns that were poorly reproducible;

Table 1. Crystallographic Summary

crystal contents	MycF WT	MycF WT	MycF WT
	Mg - disordered lid	Mg, SAH	mycinamcin III (2), Mg, SAH
	Data		
space group	C2	P2 <sub>1</sub> 2 <sub>1</sub> 2 <sub>1</sub>	P2 <sub>1</sub> 2 <sub>1</sub>
cell lengths (Å)	123.9 148.6 66.9	50.1 89.9 127.7	49.9 90.9 128.6
angles (deg)	90 120.2 90		
<i>d</i> <sub>min</sub> (Å)	2.50 (2.50–2.49) <sup>a</sup>	2.40 (2.49–2.40)	1.65 (1.68–1.65)
<i>I</i> / $\sigma$	13.3 (2.1)	15.1 (2.9)	12.6 (2.1)
<i>R</i> <sub>sym</sub>	0.080 (0.540)	0.114 (0.572)	0.073 (0.588)
multiplicity	5.8 (5.8)	6.4 (5.9)	3.6 (3.6)
completeness	100.0 (100.0)	98.4 (89.1)	99.4 (99.3)
no. of unique reflections	36246	22836	71066
	Refinement		
<i>R</i> <sub>work</sub> / <i>R</i> <sub>free</sub>	0.198/0.226	0.233/0.273	0.150/0.178
RMSD bonds (Å)	0.009	0.006	0.009
RMSD angles (deg)	1.189	0.961	1.164
Ramachandran (%)			
allowed	99.48	100	99.14
outliers	0.52	0	0.86
average B-factors (Å <sup>2</sup> )			
protein	55.0	56.7	16.7
ligands/ions	49.3	56.0	28.7
water	48.6	49.6	25.9
PDB	4XVZ	4XVY	4X7U
crystal contents	MycF E35Q E139A	MycF E35Q E139A	MycF E35Q E139A
	mycinamicin IV (3), Mg, SAH	macrocin (6), Mg, SAH	mycinamcin VI (1), Mg, SAH
	Data		
space group	P2 <sub>1</sub> 2 <sub>1</sub> 2 <sub>1</sub>	P2 <sub>1</sub> 2 <sub>1</sub> 2 <sub>1</sub>	P2 <sub>1</sub> 2 <sub>1</sub> 2 <sub>1</sub>
cell lengths (Å)	50.1 92.4 128.5	50.2 91.6 128.4	50.3 91.9 128.3
angles (deg)			
<i>d</i> <sub>min</sub> (Å)	1.45 (1.54–1.45)	1.75 (1.85–1.75)	1.45 (1.50–1.45)
<i>I</i> / $\sigma$	19.2 (3.2)	13.6 (4.9)	22.0 (4.2)
<i>R</i> <sub>sym</sub>	0.055 (0.40)	0.085 (0.379)	0.119 (0.591)
CC <sub>1/2</sub> (%)	99.9 (90.9)	99.8 (96.8)	
multiplicity	6.7 (4.2)	7.3 (7.2)	6.9 (6.1)
completeness	92.4 (63.7)	97.0 (99.5)	93.0 (94.9)
no. of unique reflections	99022	60579	105396
	Refinement		
<i>R</i> <sub>work</sub> / <i>R</i> <sub>free</sub>	0.159/0.181	0.163/0.200	0.180/0.209
RMSD bonds (Å)	0.007	0.006	0.010
RMSD angles (deg)	1.437	1.154	1.427
Ramachandran (%)			
allowed	100	100	99.58
outliers	0	0	0.42
average B-factors (Å <sup>2</sup> )			
protein	15.7	16.8	21.2
ligands/ions	22.4	27.3	32.0
water	29.3	28.1	32.0
PDB	4X7V	4X7X	4X7W
crystal contents	MycF/E35Q/M56A/E139A	MycF/E35Q/M56A/E139A	MycF/E35Q/M56A/E139A
	Mg, SAH	mycinamicin III (2), Mg, SAH	mycinamcin VI (1), Mg, SAH
	Data		
space group	P2 <sub>1</sub> 2 <sub>1</sub> 2 <sub>1</sub>	P2 <sub>1</sub> 2 <sub>1</sub> 2 <sub>1</sub>	P2 <sub>1</sub> 2 <sub>1</sub> 2 <sub>1</sub>
cell lengths (Å)	50.4 89.9 128.7	50.4 92.5 127.8	50.3 91.8 127.8
angles (deg)			
<i>d</i> <sub>min</sub> (Å)	1.40 (1.48–1.40)	1.44 (1.53–1.44)	1.59 (1.69–1.59)
<i>I</i> / $\sigma$	12.9 (0.9)	11.6 (1.4)	12.9 (2.0)
<i>R</i> <sub>sym</sub>	0.072 (0.901)	0.077 (0.561)	0.078 (1.03)
CC <sub>1/2</sub> (%)	99.8 (50.7)	99.9 (80.8)	99.9 (87.9)
multiplicity	6.5 (3.3)	5.8 (3.1)	6.6 (6.6)
completeness	85.5 (43.7)	99.0 (93.6)	98.5 (96.7)

Table 1. continued

crystal contents	MycF/E35Q/MS6A/E139A	MycF/E35Q/MS6A/E139A	MycF/E35Q/MS6A/E139A
	Mg, SAH	mycinamicin III (2), Mg, SAH	mycinamicin VI (1), Mg, SAH
	Data		
no. of unique reflections	99384	107004	79006
	Refinement		
$R_{\text{work}}/R_{\text{free}}$	0.166/0.189	0.161/0.178	0.175/0.195
RMSD bonds (Å)	0.007	0.010	0.008
RMSD angles (deg)	1.251	1.467	1.354
Ramachandran (%)			
allowed	100	100	100
outliers	0	0	0
average B-factors (Å <sup>2</sup> )			
protein	18.7	13.7	19.0
ligands/ions	14.8	18.7	33.2
water	31.9	27.2	32.1
PDB	4X7Y	4X7Z	4X81

<sup>a</sup>Values in parentheses refer to the highest resolution shell.

however, screening hundreds of crystals yielded structures of the free enzyme, the binary SAH complex, and the ternary substrate complex. We improved crystal quality by engineering a double-substituted variant (E35Q/E139A) that crystallized reproducibly, had nonstreaky diffraction, and led to high-resolution structures of several ternary complexes. The double substitution had no impact on catalytic activity in end-point experiments (Table 2).

Table 2. Relative Activity of MycF Variants

MycF variant	% activity with MycF substrate (mycinamicin III, 2)
wild type	100 ± 25
D191A	5 ± 5
D191N	6 ± 6
MS6A	301 ± 20
F118Y	11 ± 3
L143A	183 ± 22
L143S	260 ± 46
L143N	194 ± 12
L143Q	33 ± 15
MS6A/L143A	135 ± 5
MS6A/L143S	68 ± 5
MS6A/L143N	66 ± 4
E35Q/E139A	128 ± 52

**Overall Structure.** MycF has a Rossmann-like fold common among small-molecule methyltransferases (Figure 2a and Supporting Information Figure 1) and, as expected, a nearly identical structure to NovP (RMSD of 0.41 Å for 203 Cα atoms, 54% sequence identity).<sup>5,23</sup> Both in solution and in crystals, MycF is a dimer with an N-terminal helix (residues 6–19) at the subunit interface (Figure 2b). A metal ion is bound in the active site in all crystal structures, and an active site lid is formed by an N-terminal “lid loop” (residues 25–51) as well as an α-helical “lid domain” (residues 116–144; Figure 2d).

**Substrate Binding Orders the Active site Lids.** The active site of MycF becomes progressively more ordered as the cosubstrate and substrate bind. In the free enzyme, both parts of the active site lid are disordered (Figure 2c). SAM/SAH binding to MycF closes the helical lid domain over the cosubstrate, partially orders the lid loop, and forms the binding site for the substrate mycinamicin III (2, Figure 2d), which

orders the remainder of the lid loop (Figure 2e). In contrast to the full assembly of the MycF active site, the NovP/SAH complex has a partially disordered lid loop and no metal ion.<sup>23</sup> The ordering upon SAM binding fully buries the cosubstrate inside MycF, consistent with the reported ordered bi-bi mechanism of TylF, a MycF homologue where cosubstrate exchange is the first and last step in the catalytic cycle.<sup>24</sup>

The ordered lid loop and helical lid domain form a funnel-shaped substrate-entry channel with Mg<sup>2+</sup> and SAM at the bottom. The substrate binds with the javose sugar at the narrow bottom of the funnel (8 Å wide). The macrolactone core rests in the tapered upper portion of the funnel, which is 10 × 20 Å at its widest and is formed by several hydrophobic residues from the lid domain and lid loop (Figure 2g).

**Active Site Organization.** The structures of MycF provide the first view of metal binding to a MycF/TylF family member. A metal ion is bound in the active site in all crystallized states of the enzyme even though no metal was included during the final purification step. The metal is presumed to be Mg<sup>2+</sup> based on the octahedral coordination by oxygen ligands and the Mg<sup>2+</sup> dependence of MycF/TylF family members.<sup>12,22,24,25</sup> The Mg<sup>2+</sup> binds in a negatively charged pocket where there are three monodentate Asp ligands in all structures (Figure 2f). A fourth Asp (191) is also a Mg<sup>2+</sup> ligand in the SAH binary complex. Substrate hydroxyl groups or water occupy the other sites in the octahedral coordination shell.

The 3'- and 4'-hydroxyl groups of the mycinamicin III (2) javose sugar coordinate the Mg<sup>2+</sup> ion, placing the 3'-hydroxyl in position for methylation, 4.7 Å from the SAH sulfur and 3.1 Å from the modeled SAM methyl group. Gln246 also stabilizes the substrate through a hydrogen bond from the 4'-hydroxy to the amide carbonyl. In the substrate complex, the javose 3'-hydroxyl displaces Asp191 from the Mg<sup>2+</sup> ligand field and forms a hydrogen bond with the Asp carboxylate. Asp191 is conserved in the TylF/MycF family, and we hypothesized that it may be the catalytic base to deprotonate the substrate (Figure 2f). Asparagine and alanine substitutions at Asp191 impaired the methyltransfer reaction nearly 100 fold, indicating that the residue plays an important role in catalysis. (Table 2). If Asp191 indeed deprotonates the 3'-hydroxyl, then the residual activity of D191N and D191A could be due to deprotonation by an active site water molecule.

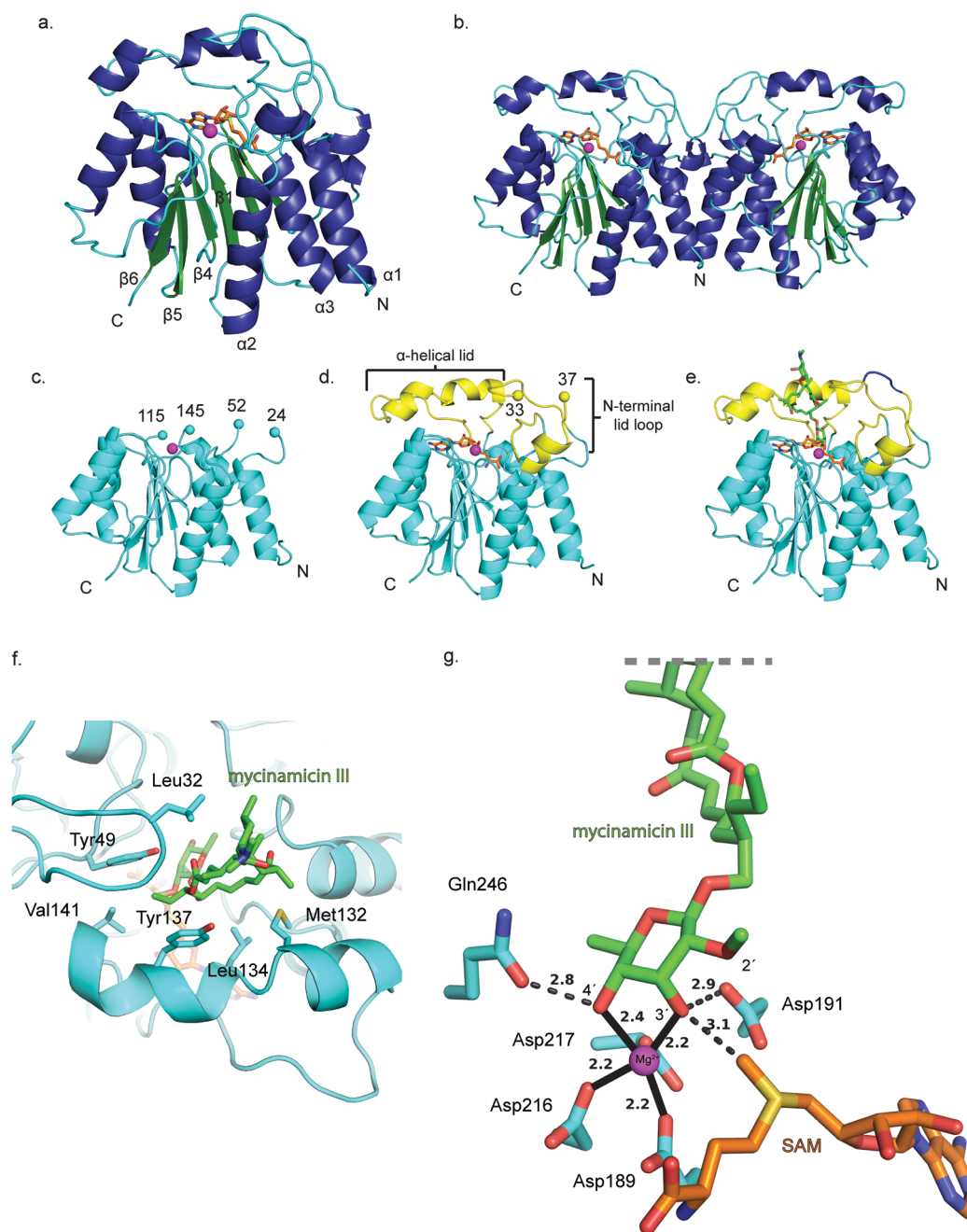


**Figure 2.** Structure of MycF. (a) MycF monomer with SAH (orange sticks) and  $Mg^{2+}$  (magenta sphere) in the active site. (b) MycF dimer with N-terminal interface. (c–e) SAM binding orders the active site lids and creates a binding pocket for mycinamicin III 2. (c) Free enzyme with disordered lid domain and lid loop and a solvent-exposed active site  $Mg^{2+}$  (magenta sphere). (d) MycF-SAH. The lid domain (yellow) closes over the bound cosubstrate, and the lid loop is partially ordered. (e) MycF-SAH-substrate. Mycinamicin III (2, green sticks) binding fully orders the lid loop (dark blue). Spheres mark the boundaries of disordered regions. MycF is specific for the javose sugar and makes no specific contacts with the macrolactone ring or desosamine sugar. (f) Hydrophobic interactions of MycF with the substrate macrolactone core. View is orthogonal to c–e. (g) Substrate binding. Three Asp residues coordinate  $Mg^{2+}$ .  $Mg^{2+}$  coordination of the mycinamicin III 2 3'- and 4'-hydroxy groups position the substrate for catalysis. The SAM methyl group (modeled) is 3.1 Å from the 3'-hydroxy. Asp191 is positioned to act as the catalytic base.

**Comparison to Related Methyltransferases.** MycF has an active site similar to those of other metal-dependent O-methyltransferases (OMT), including catechol OMT,<sup>31</sup> alfalfa caffeoyl coenzyme A 3-OMT,<sup>32</sup> the TDP-rhamnose 3-OMT CalS11,<sup>28</sup> the novobiocin 4'-OMT NovP,<sup>23</sup> and the mycinamicin 2'-OMT MycE.<sup>20</sup> These metal-dependent OMTs share a conserved SAM binding site, metal binding site, and catalytic base position (Lys in catechol OMT and caffeoyl CoA OMT, His in MycE, and Asp in CalS11, NovP, and MycF.) In all

cases,  $Mg^{2+}$  coordinates adjacent substrate hydroxyl groups and positions the target hydroxy for methylation by SAM. Despite the common structures of their active sites, these enzymes are from distant branches of the class-I methyltransferase family with highly divergent sequences, quaternary structures, and decorations on the common methyltransferase fold.<sup>5</sup> Among this group, MycF is closely related only to NovP. Beyond the fold of the catalytic core, MycF has no sequence similarity and little structural similarity to RebM, a nonmetal dependent

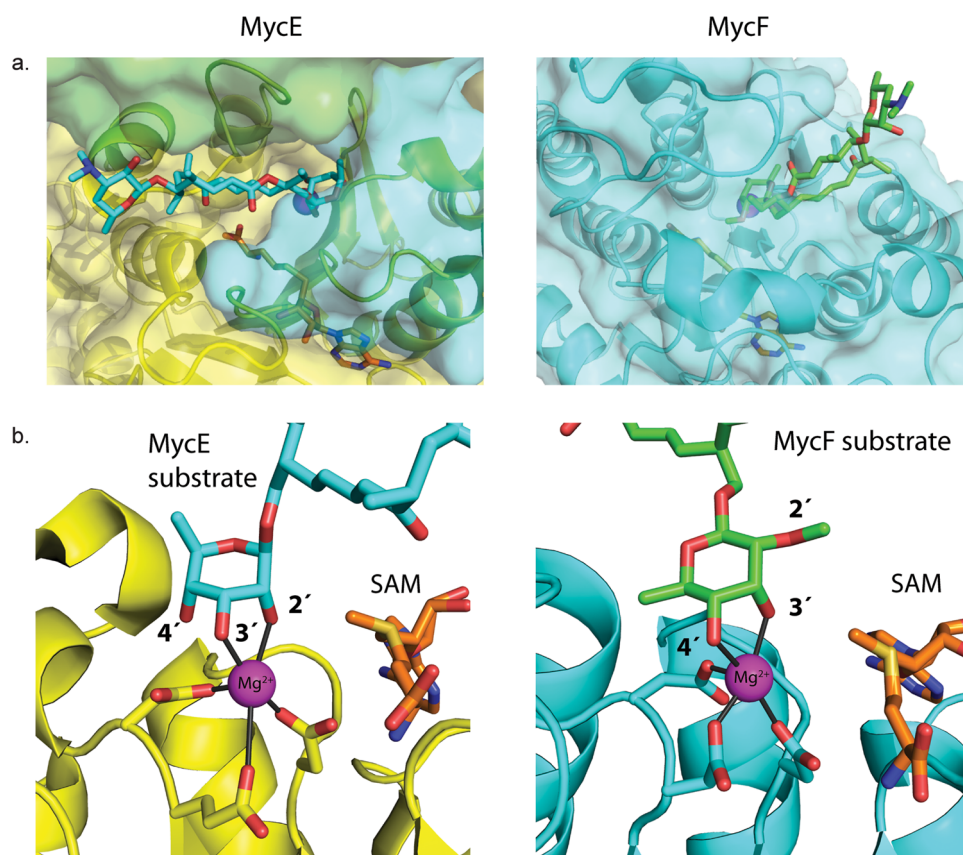


**Figure 3.** Comparison of MycE and MycF active sites. (a) Surface representation. The active site of MycE (ref 20; 3SSN, left) is at the intersection of three subunits (yellow, green, cyan) whereas the MycF (right; cyan) substrate binds to a single subunit. The MycE and MycF active site lids direct substrate (cyan, green) entry on opposite sides of the catalytic  $Mg^{2+}$  (magenta) and SAM (orange), shown in identical orientations. (b) MycE (yellow) and MycF (cyan) active sites. The different substrate orientations result in different sugar conformations, sugar coordination of  $Mg^{2+}$ , and regiochemistry of methylation.

natural product sugar *O*-methyltransferase. This is not surprising given the structural diversity of small-molecule methyltransferases.

It is of interest to compare the mycinamicin 2'-OMT MycE<sup>20</sup> and the 3'-OMT MycF, as they provide the first view of ordered sugar methylation in macrolide biosynthesis. Despite their common active site structures, MycF and MycE have substantially different substrate positions (Figure 3a). In MycE, the substrate (1) 2'- and 3'-hydroxyls coordinate  $Mg^{2+}$  with the sugar in a chair conformation with four axial substituents and the 2'-hydroxy proximal to the SAM methyl. In contrast, in MycF the substrate 3'- and 4'-hydroxyl groups coordinate  $Mg^{2+}$  with the sugar in a different chair conformation with only one axial substituent, and the 3'-hydroxyl near the SAM methyl (Figure 3b). Although the MycE substrate conformation appears less favorable (four axial substituents vs. one), the calculated free energy difference between these two substrate poses is only 23.9 kJ/mol (5.7 kcal/mol). This can be rationalized by the  $Mg^{2+}$  coordination bonds and hydrophobic interactions of the macrolactone core, which are more extensive with MycE than with MycF.<sup>20</sup>

**Substrate Selectivity.** The MycF ternary complex with SAH and the natural substrate mycinamicin III 2 suggests that MycF may be active with alternative substrates. The macrolactone is located in a hydrophobic region at the opening of the active site funnel (Supporting Information Figure 2a) where it is partially solvent-exposed and forms no specific contacts with MycF (Figure 2g). The terminal desosamine sugar is less well

ordered, makes no protein contacts, and does not appear to contribute to substrate specificity. Thus, MycF might accept javose substrates bearing different macrolactones, differentially substituted macrolactones, or nonmacrolactone hydrophobic substituents.

To assess the flexibility of MycF to accept alternative substrates, we examined the activity of MycF with macrocin 6, the javose-containing intermediate in tylosin biosynthesis. Macrocin 6 is a 16-membered ring macrolide bearing javose and desosamine sugars with an additional mycarose sugar (Figure 1b). In our standard assay conditions, MycF methylated the 3' hydroxyl of macrocin 6 to produce the macrolide antibiotic tylosin (Supporting Information Figure 3), confirming that MycF tolerates changes to the macrolactone core. As seen in the SAH-macrocin 6 ternary complex, the differences in the macrolactone structure do not alter the position of javose in the active site (Supporting Information Figure 2d).

**Pathway Ordering.** A key motivation for our study was to understand the structural basis for the specific order of sugar hydroxyl group methylation in the biosynthesis of mycinamicin and tylosin<sup>12,21,24,25</sup> in which members of the MycF subfamily methylate the 3'-hydroxyl only after methylation of the 2'-hydroxyl of 6'-deoxyallose (creating the javose moiety). How does MycF distinguish the substrate mycinamicin III 2 from mycinamicin VI 1, which is not a substrate,<sup>12</sup> as these molecules differ only in the 2' substituent (methoxy vs hydroxy)? It was

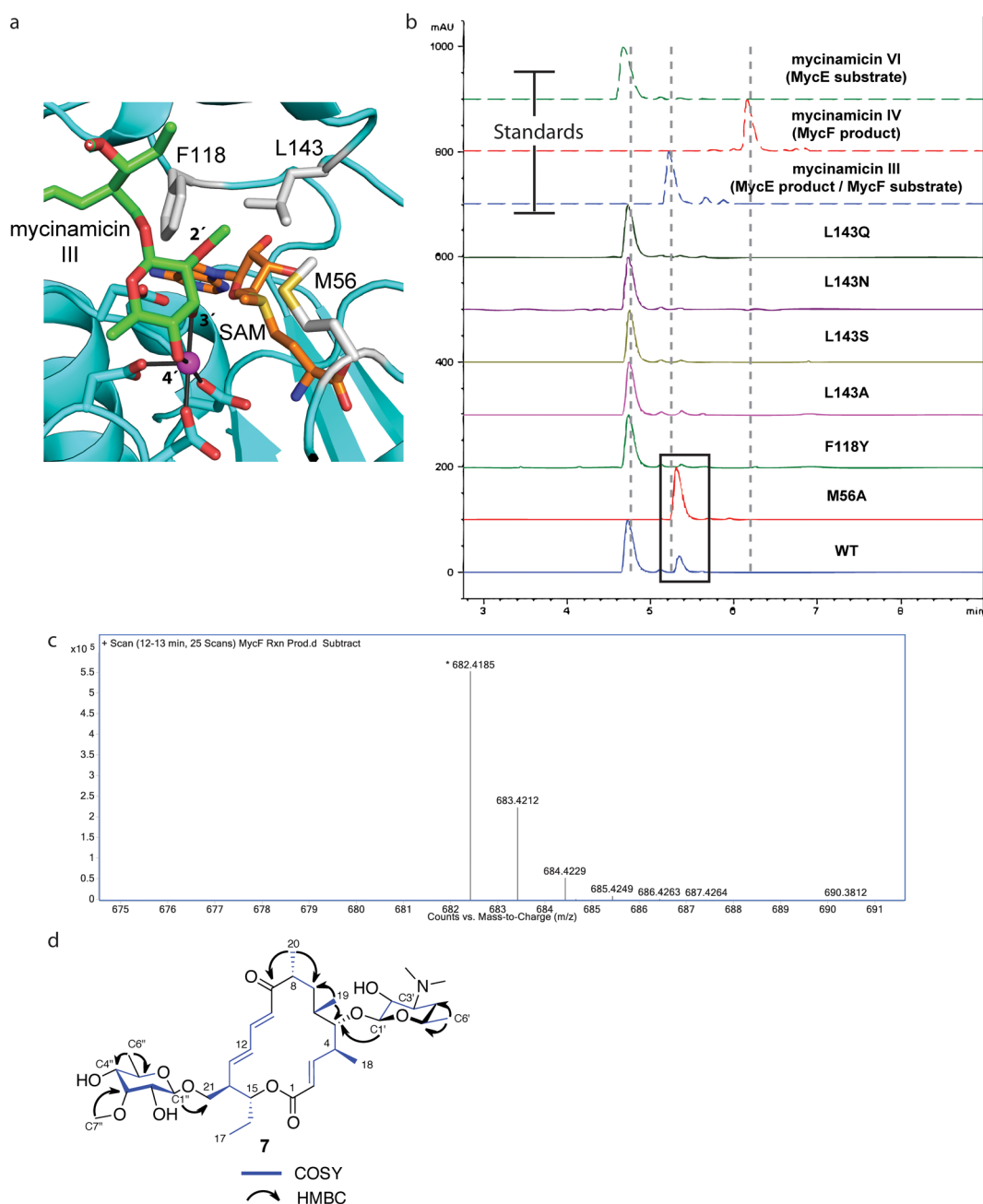


**Figure 4.** MycF activity with MycE substrate (mycinamicin VI **1**). (a) MycF active site with 2'-methoxy specificity pocket. Residues selected for substitution experiments are shown in gray sticks. (b) HPLC chromatograms of MycF variants with the MycE substrate (mycinamicin VI **1**). Wild type MycF and MycF/M56A show production of a new product that has a retention time similar to mycinamicin III **2**. (c) Mass spectrum of HPLC-purified product of MycF/M56A reaction with the MycE substrate. The M+H peak for the product has a mass comparable to that for the MycE product (monoisotopic mass of mycinamicin III **2** 681.4 Da compared to 682.4 Da for the M+H peak). (d) Structure of 3'-methoxy-mycinamicin VI **7**. COSY and HMBC correlations are indicated; NMR spectra are in the Supporting Information.

not immediately apparent from the structures why MycF does not methylate the MycE substrate mycinamicin VI **1**.

The javose 2'-methoxy binds in a hydrophobic pocket created by Met56, Phe118, Leu143, and Val141 (Figure 4a). Reasoning that this pocket might be too hydrophobic for a 2'-hydroxyl group, we substituted alanine or a polar side chain for each of three hydrophobic amino acids in the pocket (Met56, Phe118, Leu143). None of the variants had detectable activity with mycinamicin VI **1** under standard assay conditions although, interestingly, four of the substitutions increased activity with the natural substrate mycinamicin III **2** in our end

point assay (Table 2). Several double-substituted MycF variants lacked synergistic or additive effects in the end point assay with the natural substrate **2**, and no activity was observed with the MycE substrate **1** in the standard assay (Table 2). Steady state kinetic constants were similar for the wild type ( $K_m$   $10.9 \pm 2.9 \mu\text{M}$ ,  $V_{\text{max}}$   $0.08 \pm 0.01 \mu\text{Ms}^{-1}$ ,  $k_{\text{cat}}$   $0.27 \text{ s}^{-1}$ ) and the M56A variant ( $K_m$   $6.4 \pm 1.8 \mu\text{M}$ ,  $V_{\text{max}}$   $0.04 \pm 0.002 \mu\text{Ms}^{-1}$ ,  $k_{\text{cat}}$   $0.13 \text{ s}^{-1}$ ). However, the wild type MycF had decreased initial velocity at high substrate concentrations, suggestive of substrate inhibition, whereas the M56A variant exhibited no substrate inhibition and thus appeared "hyper-active" (Supporting

Information Figure 4). As SAM/SAH binds beneath the substrate (Figure 2e), we hypothesize that at high substrate concentrations, product release is followed by new substrate binding faster than SAM replaces SAH in the active site. Substrate (or product) binding stabilizes the fully closed conformation of the active site lid (Figure 2e), which may slow both cosubstrate exchange and the rate of catalysis, explaining the observed greater activity of M56A in the end point assay (Table 2). Met56 is adjacent to SAM (Figure 4a), and substitution with Ala may allow SAH/SAM exchange in the presence of substrate or product.

Remarkably, the crystal structure of MycF in a ternary complex with SAH and the MycE substrate shows that mycinamicin VI **1** binds similarly to the authentic MycF substrate mycinamicin III **2** with 3'- and 4'-hydroxy coordination of Mg<sup>2+</sup> (Supporting Information Figure 2c). However, the sugar is shifted ~1 Å deeper into the binding pocket and rotated ~15° toward SAM (Supporting Information Figure 5a), positioning the polar 2'-hydroxyl group outside the hydrophobic methoxy binding pocket. The Met56 side chain appears to exclude the authentic substrate from this position by a steric clash with the 2'-methoxy. Residual positive  $F_o - F_c$  electron density indicates that the sugar samples multiple conformations. The predominant position is incompatible with the SAM methyl group (~2.6 Å from the 3'-hydroxy and ~2.7 Å from the 2'-hydroxy, Supporting Information Figure 5b,c). Thus, mycinamicin VI **1** may be excluded from the MycF active site when SAM is bound, or it may bind in a nonproductive position in the presence of SAM.

**Generation and Characterization of a New Mycinamicin Compound.** The binding pose of the MycE substrate in the MycF active site suggests that MycF should methylate the MycE substrate, despite the lack of activity under standard assay conditions. At high concentrations, MycF converted approximately 10% of mycinamicin VI **1** (MycE substrate) to a previously unreported product (Figure 4b). Under the same conditions, the M56A variant exhibited 100% conversion of mycinamicin VI to the new product (Figure 4b) with a mass relative to the starting material consistent with a single methylation (+14 Da, Figure 4c) but a slightly different HPLC retention time than the singly methylated mycinamicin III product of MycE (Figure 4b). We confirmed with multidimensional NMR that the product is 3'-methoxy-mycinamicin VI **7**, a new mycinamicin analog methylated at the 3'-hydroxy (but not the 2'-hydroxy; Table 3, Figure 4d, and Supporting Information). Remarkably, the engineered enzyme had reduced substrate selectivity but retained regiospecificity; *i.e.* each substrate produced only a single product. These results demonstrate the potential utility of the MycF M56A variant in engineered production strains. Although the variant does not exhibit increased catalytic efficiency relative to the wild type, the decrease in substrate inhibition results in increased product formation over time.

MycF/M56A binds Mg<sup>2+</sup> and SAH identically to the wild type, but both substrates, mycinamicin III and mycinamicin VI (Supporting Information Figure 6), occupy the deep position observed in wild type MycF for the MycE substrate. The position of the Met56 side chain is occupied by a DMSO molecule (mycinamicin solvent) in the mycinamicin VI complex (Supporting Information Figures 5d and 7) and by the 2'-methoxy in the mycinamicin III complex. The position of both substrates is incompatible with the SAM cosubstrate; therefore both substrates must move in the substrate-SAM

**Table 3. Chemical Shift Assignments for 3'-Methoxymycinamicin VI**

atom	$\delta_C$	$\delta_H$ , multi (J in Hz)	COSY	HMBC
1				
2	121.5	5.93, d (15.4)	3	
3	151.4	6.54, dd (10.1, 15.4)	2, 4	
4	41.7	2.76, m	3, 5, 18	
5	88	3.36, m	4	
6	34	1.22, m	19	
7	33.18	1.72, m	8	
8	45.3	2.47, m	7, 20	
9	203.1			
10	123.7	6.46, d (15.0)	11	
11	141.2	7.01, dd (10.9, 15.0)	10, 12	
12	133.5	6.24, dd (10.9, 15.4)	11, 13	
13	141.2	6.02, dd (9.3, 15.4)	12	
14	49.3	2.49, m	13, 15, 21	
15	74.1	4.91, m	14, 16	
16	23.6	1.59, m	15, 17	
17	9.7	0.9, t (7.3, 14.6)	16	
18	19.4	1.23, d (6.7)	4	
19	17.6	0.99, d (6.8)	6	5, 7
20	17.7	1.14, d (7.0)	8	7, 9
21	68.4	3.68, m	14	
C1'	105.7	4.28, d (7.3)	C2'	5
C2'	70	3.16, dd (7.3, 9.8)	C1', C3'	
C3'	66.5	2.53, m	C2', C4'	
C4'	29.56	1.74, m	C3'	
C5'	69.5	3.55, m		
C6'	21.2	1.18, d (3.2)	C5'	C5', C4'
N(CH <sub>3</sub> ) <sub>2</sub>	40.4	2.29, m		C3', N(CH <sub>3</sub> ) <sub>2</sub>
C1''	101.9	4.5 d, (7.8)	C2''	21
C2''	72.7	3.41, m	C1', C3'	
C3''	82.6	3.65, m	C2'', C4''	
C4''	73.9	3.18, m	C3'', C5''	
C5''	70.9	3.15, m	C4''	
C6''	17.9	1.19, d (3.2)		C4'', C5''
C7''	61.7	3.58, m		C3''

complex. The hydrophobic 2'-methoxy substituent in the authentic substrate can engage other surfaces of the hydrophobic pocket that are less accommodating to a 2'-hydroxy substituent, explaining the difference in activity of MycF/M56A on the two substrates.

Enzymatic production of 3'-methoxy-mycinamicin VI allowed us to test for the first time whether MycE can accept substrates with a 3'-methoxy sugar. MycE was unable to produce the doubly methylated mycinamicin IV **3** from 3'-methoxy-mycinamicin VI **7** (Supporting Information Figure 8). A hydrogen bond between the mycinamicin VI 3'-hydroxy and MycE His180 (ref 20, 3SSN) selects the 3'-hydroxy substrate. These results demonstrate how both MycE and MycF contribute to reaction ordering in the tailoring steps of macrolide biosynthesis. The importance of this ordering is underscored by the observation that the MycG monooxygenase that completes mycinamicin biosynthesis requires both the 2'- and 3'-methoxy groups on the mycinose sugar.<sup>33</sup>

**Regiospecificity in MycF/TyIF Family Members.** Proteins in the MycF/TyIF/NovP subfamily of the class-I methyltransferases have high sequence identity (~50% or greater) and are expected to have structures as similar to MycF as is NovP (0.4 Å rmsd, 54% identity). Thus, the structures of

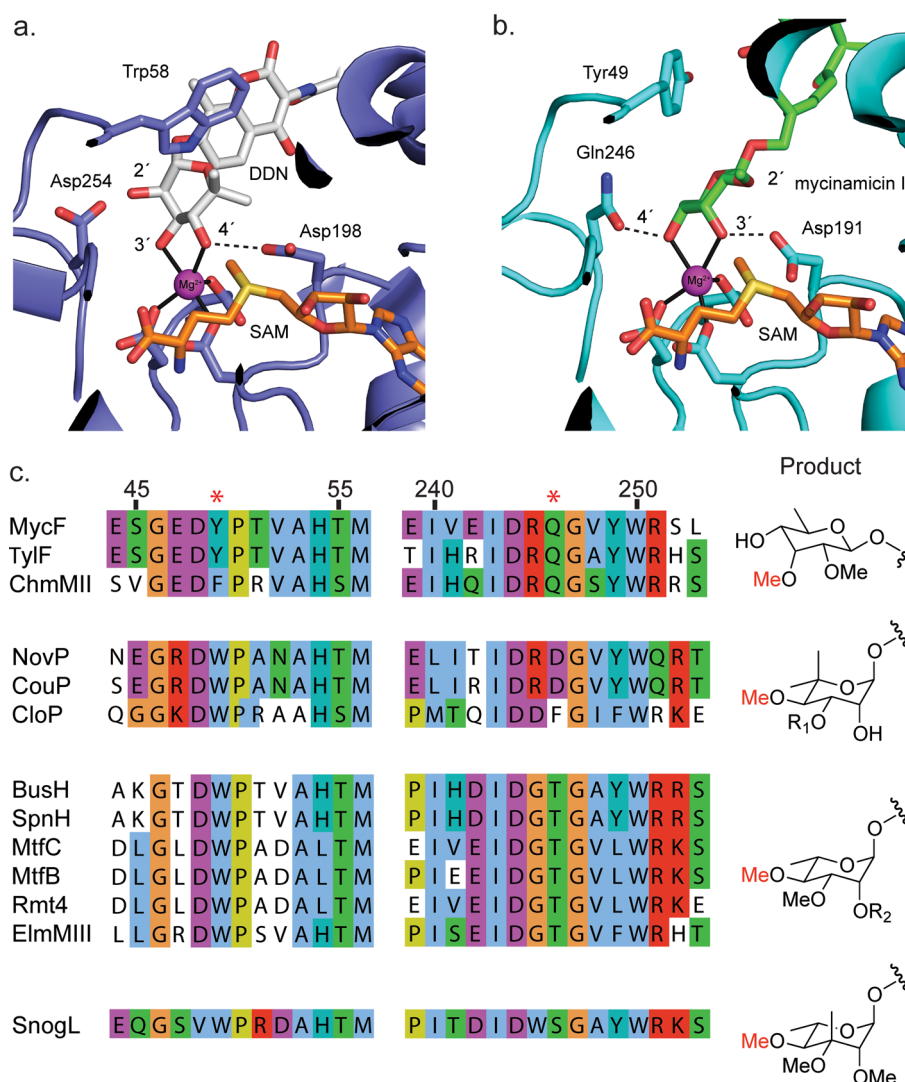


**Figure 5.** Regiochemistry of methyltransfer in MycF homologues. (a) Model of NovP substrate complex. The NovP 4'-O-MT is in dark blue, substrate DDN 5 in gray, and SAM in orange. (b) Structure of MycF-substrate complex with MycF in cyan, mycinamicin III 2 in green, and SAM in orange. (c) Partial sequence alignment of MycF homologues (MycF numbering). All MycF/TylF family members with known substrates are grouped based on the product sugar, shown at right. Tryptophan at position 49 is strictly conserved among 4'-specific enzymes, as is glutamine at position 246 in 3'-specific enzymes. The conserved tryptophan contributes to the hydrophobic pocket for the 5'-methyl group (shown in a). MycF, mycinamicin 3'-O-methyltransferase;<sup>34</sup> TylF, tylosin 3'-O-methyltransferase;<sup>35</sup> ChmMII, chalcocycin 3'-O-methyltransferase;<sup>18</sup> NovP, novobiocin 4'-O-methyltransferase;<sup>17</sup> CouP, coumestrol 4'-O-methyltransferase;<sup>17</sup> CloP, clorobiocin 4'-O-methyltransferase;<sup>14</sup> BusH, butenyl-spinosyn 4'-O-methyltransferase;<sup>13</sup> SpnH, spinosyn 4'-O-methyltransferase;<sup>16</sup> MtfC, *Mycobacterium avium* glycopeptidolipid 4'-O-methyltransferase; MtfB, *Mycobacterium avium* glycopeptidolipid 4'-O-methyltransferase; Rmt4, *Mycobacterium chelonae* glycopeptidolipid 4'-O-methyltransferase; ElmMIII, elloramycin 4'-O-methyltransferase;<sup>19</sup> SnogL, nogalamycin 4'-O-methyltransferase.<sup>15</sup>

subfamily members and their active sites can be modeled with a high degree of confidence. The 13 experimentally characterized subfamily members are sugar 3'- and 4'-OMTs that act after the glycosyltransfer step in the biosynthesis of secondary metabolites. We modeled the substrate complex for the 4'-OMT NovP (2WK1),<sup>23</sup> the only other subfamily member of known structure. The substrate DDN (5) was manually positioned in the NovP active site constrained by the methylation site and  $Mg^{2+}$  coordination geometry of MycF (Figure 5a). The lid loop of MycF guided positioning of the DDN (5) aminocoumarin, as the corresponding residues are disordered in the NovP structure. Positioning the 4'-hydroxy for methylation and the 3'-hydroxy as a  $Mg^{2+}$  ligand required that the novobiose sugar be flipped in the active site relative to the orientation of javose in MycF (Figure 5a,b). The novobiose

sugar makes no specific contacts with amino acids apart from the Asp191 putative catalytic base. The strict regiospecificity of the sugar OMTs results from the relative positions of the hydrophobic macrolactone binding site, metal site, and metal ligands that position the substrate 3'- or 4'-hydroxy near the SAM methyl.

With MycF (3'-OMT) and NovP (4'-OMT) as prototypes, we grouped the aligned sequences of the 13 experimentally characterized subfamily members based upon the substrate structures and sites of methylation (Figure 5c). Two amino acids correlate with the regiospecificity of methyl transfer and interact with the substrate in the MycF structure and NovP model. MycF Gln246 forms a hydrogen bond with the sugar 4'-hydroxy and is conserved among the 3'-OMTs, all of which have sugar 4'-hydroxyl substrates. The Gln246 interaction

excludes substrates with 4'-alkoxy substituents. A smaller polar amino acid (Asp or Thr) occupies the analogous position in the 4'-specific enzymes. NovP Trp58, conserved in the 4'-specific enzymes, forms a hydrophobic pocket for the 5'-methyl substituent in all known substrates of the 4'-OMTs. The 3'-specific enzymes have a conserved tyrosine or phenylalanine at the analogous position (Tyr49 in MycF). Given the variability of the substrate sugars, the strict correlation of these two amino acids with the regioselectivity of the enzymes is striking and will be useful in the identification and annotation of new natural product biosynthetic pathways.

On the basis of the MycF structures and NovP model, we propose guidelines to predict the substrate specificity and regioselectivity of the several dozen MycF/TylF family members with uncharacterized activities (Figure 5). MycF is selective for substrates with 3' and 4' *syn*-hydroxyl groups that are on the opposite face of the sugar from the glycosidic bond, as found in the mycinose sugar of mycinamicin or tylosin. Although methoxy groups can serve as metal ligands, as observed in the MycF product (mycinamicin IV, **3**) complex, MycF cannot accommodate 4'-methoxy groups in the active site. In contrast, NovP requires *anti*-hydroxyl groups at the 3' and 4' positions like those in rhamnose and also requires that the methylation site and glycosidic bond occur on the same face of the sugar ring. Further, NovP and related 4'-O-methyltransferases can accommodate 3'-methoxy substituents as Mg<sup>2+</sup> ligands, consistent with the 2',3',4'-hydroxyl group methylation order in the spinosyn pathway.<sup>21</sup>

We determined a series of structures that provide insight into the substrate specificity, mechanism, and regiochemistry of a common subfamily of sugar O-methyltransferases. The location of the 16-membered macrolactone ring and open active site suggests that this subfamily of methyltransferases may accept a variety of hydrophobic substrates bearing sugar moieties. On the basis of the substrate complex, we propose a model of the substrate position in 4'-specific members of this subfamily and identify key amino acids that can be used in the annotation of new biosynthetic pathways.

The MycF structures allowed us to identify an amino acid substitution that decreased substrate inhibition and relaxed the 2'-methoxy specificity to produce a new mycinamicin analog, while maintaining the regioselectivity of the enzyme. This is the first example of the rational engineering of a natural product sugar O-methyltransferase and demonstrates the utility of a structure-guided approach to producing new compounds. MycF variants with decreased substrate inhibition could be used in the development of high-yield strains for production-scale fermentation of macrolide antibiotics with the mycinose sugar including mycinamicins or tylosin. The synergistic use of structural information on glycosyltransferases and sugar-modifying enzymes including the MycE and MycF families of sugar O-methyltransferases will enable their use for chemo-enzymatic synthesis of novel complex natural product analogues.

## METHODS

**Protein Expression, Purification, and Mutagenesis.** Recombinant expression of native MycF has been described previously.<sup>12</sup> The single substitution variants were made with the Quik Change II Site-Directed Mutagenesis Kit (Stratagene) and the E35Q/E139A double mutant with the QuikChange Lightning Multi Site Directed Mutagenesis Kit (Stratagene) following the manufacturer's protocols (forward and reverse

primers in Supporting Information Table 1). MycF variants were expressed and purified in the same manner as WT MycF.

**Crystallization.** Initial crystals of MycF were grown by hanging-drop vapor diffusion with a 1:1 ratio of protein solution (10 mg mL<sup>-1</sup> MycF in 20 mM Tris 8.0, 150 mM NaCl 10% glycerol, 1 mM SAH) and well solution (20–30% PEG 3350, 100 mM BisTrisPropane pH 6.5). These crystals were used to solve structures of the apo enzyme, SAH binary complex, and SAH substrate ternary complex. Crystals of MycF E35Q/E139A were grown using a well solution containing 20–30% PEG 5000 MME, 100 mM ammonium acetate, and 100 mM BisTrisPropane pH 6.5. These crystals were used to solve structures of MycF in complex with mycinamicin IV **3**, mycinamicin VI **1**, and macrocin **6** and to redetermine the two previously solved complex structures. Apart from the double substitution, the redetermined structures were of similar quality and identical to the wild type complex structures. Crystals of the E35Q/M56A/E139A variant were grown under the same conditions as the E35Q/E139A variant by microseeding. For the mycinamicin III **2**, mycinamicin IV **3**, mycinamicin VI **1**, and macrocin **6** complexes, the crystals were soaked 4–6 h in well solution with 10 mM ligand. Crystals were harvested on MicroMesh mounts (MiTeGen), cryoprotected in well solution plus 10% glycerol and flash cooled in liquid N<sub>2</sub>.

**Enzyme Assays.** The end point assay was done according to published protocol<sup>12</sup> with a 100  $\mu$ L reaction mix containing 50 mM Tris buffer (pH 8.0), 5  $\mu$ M MycF, 250  $\mu$ M substrate **2**, 10 mM MgCl<sub>2</sub>. The reaction was initiated by the addition of 750  $\mu$ M SAM, incubated 30 min at 30 °C, and quenched by the addition of 100  $\mu$ L methanol. Mycinamicin VI **1** reactions were performed in the same manner with 20  $\mu$ M MycF and incubated 20 h. MycE reactions were performed under the same conditions with 5  $\mu$ M MycE in place of MycF. Precipitated protein was removed by centrifugation, and the components of the reaction mixture were separated by reverse phase HPLC; absorbance was monitored at 280 nm. Integrated peak areas for the substrate and product were used to calculate percent conversion and normalized to the wild type MycF activity. Reactions were performed in triplicate. Components of reaction mixtures were validated with authentic standards of mycinamicin VI **1**, mycinamicin III **2**, and mycinamicin IV **3**. The product of the MycF reaction with mycinamicin III **2** and SAM has been characterized by LC-MS and reported previously.<sup>12</sup>

## ASSOCIATED CONTENT

### Supporting Information

Supporting Information methods, tables, and figures. This material is available free of charge via the Internet at <http://pubs.acs.org>.

### Accession Codes

Atomic coordinates and structure factors have been deposited in the Protein Data Bank under the following PDB accession codes: 4XVZ (MycF), 4XVY (MycF-SAH), 4X7U (mycinamicin III complex), 4X7V (mycinamicin IV complex), 4X7W (mycinamicin VI complex), 4X7X (macrocin complex), 4X7Y (MycF/M56A-SAH), 4X7Z (MycF/M56A mycinamicin III complex), and 4X81 (MycF/M56A mycinamicin VI complex).

## AUTHOR INFORMATION

## Corresponding Author

\*E-mail: janetsmith@umich.edu.

## Notes

The authors declare no competing financial interest.

## ACKNOWLEDGMENTS

This work was supported by NIH grant DK042303 to J.L.S. and National Institutes of Health grant GM078553 and the Hans W. Vahlteich Professorship to D.H.S. S.M.B. acknowledges training grant support from the University of Michigan Chemistry–Biology Interface (CBI) training program (NIH grant 5T32GM008597). GM/CA has been funded in whole or in part with federal funds from the National Cancer Institute (Y1-CO-1020) and the National Institute of General Medical Sciences (Y1-GM-1104). Use of the Advanced Photon Source was supported by the U.S. Department of Energy, Basic Energy Sciences, Office of Science, under contract No. DE-AC02-06CH11357.

## REFERENCES

- (1) Newman, D. J., and Cragg, G. M. (2007) Natural products as sources of new drugs over the last 25 years. *J. Nat. Prod.* 70, 461–477.
- (2) Park, S. R., Han, A. R., Ban, Y. H., Yoo, Y. J., Kim, E. J., and Yoon, Y. J. (2010) Genetic engineering of macrolide biosynthesis: past advances, current state, and future prospects. *Appl. Microbiol. Biotechnol.* 85, 1227–1239.
- (3) Mortison, J. D., and Sherman, D. H. (2010) Frontiers and opportunities in chemoenzymatic synthesis. *J. Org. Chem.* 75, 7041–7051.
- (4) Hansen, D. A., Rath, C. M., Eisman, E. B., Narayan, A. R., Kittendorf, J. D., Mortison, J. D., Yoon, Y. J., and Sherman, D. H. (2013) Biocatalytic synthesis of pikromycin, methymycin, neomethymycin, novamethymycin, and ketomethymycin. *J. Am. Chem. Soc.* 135, 11232–11238.
- (5) Liscombe, D. K., Louie, G. V., and Noel, J. P. (2012) Architectures, mechanisms and molecular evolution of natural product methyltransferases. *Nat. Prod. Rep.* 29, 1238–1250.
- (6) Thibodeaux, C. J., Melancon, C. E., and Liu, H. W. (2008) Natural product sugar biosynthesis and enzymatic glycodiversification. *Angew. Chem., Int. Ed. Engl.* 47, 9814–9859.
- (7) Zhang, C., Albermann, C., Fu, X., Peters, N. R., Chisholm, J. D., Zhang, G., Gilbert, E. J., Wang, P. G., Van Vranken, D. L., and Thorson, J. S. (2006) RebG- and RebM-catalyzed indolocarbazole diversification. *ChemBioChem.* 7, 795–804.
- (8) Thibodeaux, C. J., Melancon, C. E., and Liu, H. W. (2007) Unusual sugar biosynthesis and natural product glycodiversification. *Nature* 446, 1008–1016.
- (9) Singh, S., Phillips, G. N., Jr., and Thorson, J. S. (2012) The structural biology of enzymes involved in natural product glycosylation. *Nat. Prod. Rep.* 29, 1201–1237.
- (10) Sato, S., Muto, N., Hayashi, M., Fujii, T., and Otani, M. (1980) Mycinamicins, new macrolide antibiotics 0.1. taxonomy, production, isolation, characterization and properties. *J. Antibiot.* 33, 364–376.
- (11) Anzai, Y., Salto, N., Tanaka, M., Kinoshita, K., Koyama, Y., and Kato, F. (2003) Organization of the biosynthetic gene cluster for the polyketide macrolide mycinamicin in *Micromonospora griseorubida*. *FEMS Microbiol. Lett.* 218, 135–141.
- (12) Li, S., Anzai, Y., Kinoshita, K., Kato, F., and Sherman, D. H. (2009) Functional analysis of MycE and MycF, two O-methyltransferases involved in the biosynthesis of mycinamicin macrolide antibiotics. *ChemBioChem.* 10, 1297–1301.
- (13) Hahn, D. R., Gustafson, G., Waldron, C., Bullard, B., Jackson, J. D., and Mitchell, J. (2006) Butenyl-spinosyns, a natural example of genetic engineering of antibiotic biosynthetic genes. *J. Ind. Microbiol. Biotechnol.* 33, 94–104.
- (14) Pojer, F., Li, S. M., and Heide, L. (2002) Molecular cloning and sequence analysis of the clorobiocin biosynthetic gene cluster: new insights into the biosynthesis of aminocoumarin antibiotics. *Microbiology* 148, 3901–3911.
- (15) Torkkell, S., Kunnari, T., Palmu, K., Mantsala, P., Hakala, J., and Ylihanko, K. (2001) The entire nogalamycin biosynthetic gene cluster of *Streptomyces nogalater*: characterization of a 20-kb DNA region and generation of hybrid structures. *Mol. Genet. Genomics* 266, 276–288.
- (16) Waldron, C., Matsushima, P., Rosteck, P. R., Broughton, M. C., Turner, J., Madduri, K., Crawford, K. P., Merlo, D. J., and Baltz, R. H. (2001) Cloning and analysis of the spinosad biosynthetic gene cluster of *Saccharopolyspora spinosa*. *Chem. Biol.* 8, 487–499.
- (17) Wang, Z. X., Li, S. M., and Heide, L. (2000) Identification of the coumermycin A(1) biosynthetic gene cluster of *Streptomyces rishiriensis* DSM 40489. *Antimicrob. Agents Chemother.* 44, 3040–3048.
- (18) Ward, S. L., Hu, Z. H., Schirmer, A., Reid, R., Revill, P., Reeves, C. D., Petrakovsky, O. V., Dong, S. D., and Katz, L. (2004) Chalcomycin biosynthesis gene cluster from *Streptomyces bikiniensis*: Novel features of an unusual ketolide produced through expression of the chm polyketide synthase in *Streptomyces fradiae*. *Antimicrob. Agents Chemother.* 48, 4703–4712.
- (19) Patallo, E. P., Blanco, G., Fischer, C., Brana, A. F., Rohr, J., Mendez, C., and Salas, J. A. (2001) Deoxysugar methylation during biosynthesis of the antitumor polyketide elloramycin by *Streptomyces olivaceus* - Characterization of three methyltransferase genes. *J. Biol. Chem.* 276, 18765–18774.
- (20) Akey, D. L., Li, S., Konwerski, J. R., Confer, L. A., Bernard, S. M., Anzai, Y., Kato, F., Sherman, D. H., and Smith, J. L. (2011) A new structural form in the SAM/metal-dependent O-methyltransferase family: MycE from the mycinamicin biosynthetic pathway. *J. Mol. Biol.* 413, 438–450.
- (21) Kim, H. J., White-Phillip, J. A., Ogasawara, Y., Shin, N., Isiorho, E. A., and Liu, H. W. (2010) Biosynthesis of spinosyn in *Saccharopolyspora spinosa*: synthesis of permethylated rhamnose and characterization of the functions of SpnH, SpnI, and SpnK. *J. Am. Chem. Soc.* 132, 2901–2903.
- (22) Freel Meyers, C. L., Oberthur, M., Xu, H., Heide, L., Kahne, D., and Walsh, C. T. (2004) Characterization of NovP and NovN: completion of novobiocin biosynthesis by sequential tailoring of the noviosyl ring. *Angew. Chem., Int. Ed. Engl.* 43, 67–70.
- (23) Gomez Garcia, I., Stevenson, C. E., Uson, I., Freel Meyers, C. L., Walsh, C. T., and Lawson, D. M. (2010) The crystal structure of the novobiocin biosynthetic enzyme NovP: the first representative structure for the TylF O-methyltransferase superfamily. *J. Mol. Biol.* 395, 390–407.
- (24) Bauer, N. J., Kreuzman, A. J., Dotzlaw, J. E., and Yeh, W. K. (1988) Purification, characterization, and kinetic mechanism of S-adenosyl-L-methionine: macrocin O-methyltransferase from *Streptomyces fradiae*. *J. Biol. Chem.* 263, 15619–15625.
- (25) Kreuzman, A. J., Turner, J. R., and Yeh, W. K. (1988) Two distinctive O-methyltransferases catalyzing penultimate and terminal reactions of macrolide antibiotic (tylosin) biosynthesis. Substrate specificity, enzyme inhibition, and kinetic mechanism. *J. Biol. Chem.* 263, 15626–15633.
- (26) Bruender, N. A., and Holden, H. M. (2012) Probing the catalytic mechanism of a C-3'-methyltransferase involved in the biosynthesis of D-tetronitrose. *Protein Sci.* 21, 876–886.
- (27) Singh, S., McCoy, J. G., Zhang, C., Bingman, C. A., Phillips, G. N., Jr., and Thorson, J. S. (2008) Structure and mechanism of the rebeccamycin sugar 4'-O-methyltransferase RebM. *J. Biol. Chem.* 283, 22628–22636.
- (28) Singh, S., Chang, A., Helmich, K. E., Bingman, C. A., Wrobel, R. L., Beebe, E. T., Makino, S. I., Aceti, D. J., Dyer, K., Hura, G. L., Sunkara, M., Morris, A. J., Phillips, G. N., Jr., and Thorson, J. S. (2013) Structural and Functional Characterization of CalS11, a TDP-Rhamnose 3'-O-Methyltransferase Involved in Calicheamicin Biosynthesis. *ACS Chem. Biol.* 8, 1632–1639.
- (29) Anzai, Y., Li, S., Chaulagain, M. R., Kinoshita, K., Kato, F., Montgomery, J., and Sherman, D. H. (2008) Functional analysis of

MycCI and MycG, cytochrome P450 enzymes involved in biosynthesis of mycinamicin macrolide antibiotics. *Chem. Biol.* 15, 950–959.

(30) Li, S., Tietz, D. R., Rutaganira, F. U., Kells, P. M., Anzai, Y., Kato, F., Pochapsky, T. C., Sherman, D. H., and Podust, L. M. (2012) Substrate recognition by the multifunctional cytochrome P450 MycG in mycinamicin hydroxylation and epoxidation reactions. *J. Biol. Chem.* 287, 37880–37890.

(31) Vidgren, J., Svensson, L. A., and Liljas, A. (1994) Crystal structure of catechol O-methyltransferase. *Nature* 368, 354–358.

(32) Ferrer, J. L., Zubietta, C., Dixon, R. A., and Noel, J. P. (2005) Crystal structures of alfalfa caffeoyl coenzyme A 3-O-methyltransferase. *Plant Physiol.* 137, 1009–1017.

(33) Anzai, Y., Tsukada, S., Sakai, A., Masuda, R., Harada, C., Domeki, A., Li, S., Kinoshita, K., Sherman, D. H., and Kato, F. (2012) Function of cytochrome P450 enzymes MycCI and MycG in *Micromonospora griseorubida*, a producer of the macrolide antibiotic mycinamicin. *Antimicrob. Agents Chemother.* 56, 3648–3656.

(34) Inouye, M., Suzuki, H., Takada, Y., Muto, N., Horinouchi, S., and Beppu, T. (1994) A gene encoding mycinamicin III O-methyltransferase from *Micromonospora griseorubida*. *Gene* 141, 121–124.

(35) Cundliffe, E., Bate, N., Butler, A., Fish, S., Gandeche, A., and Merson-Davies, L. (2001) The tylosin-biosynthetic genes of *Streptomyces fradiae*. *Antonie Van Leeuwenhoek* 79, 229–234.